Volume 1 | Number 1 | Jan 2013 | Pages 1–100

Nanoscale

www.rsc.org/nanoscale

ROYAL SOCIETY OF CHEMISTRY

ROYAL SOCIETY OF CHEMISTRY

www.rsc.org/nanoscale

Nanoscale

MINIREVIEW

Surface Effect in Metal Oxide-Based Nanodevices

Der-Hsien Lien, José Ramón Durán Retamal, Jr-Jian Ke, Chen-Fang Kang, and Jr-Hau He*

As the devices shrink to nanoscale, surface-to-volume ratio increases and the surface-environment interaction becomes a main factor to affect the device performance. The variation of electronic properties regarding the surface band bending, gas chemisorption or photodesorption, native surface defects, and surface roughness, are called "surface effects". Such effects are ambiguous since they can be either a negative or beneficial effects, depending on the environmental conditions and device applications. This review provides an introduction of the surface effects on different types of nanodevices, offering the solutions to response to their benefits and negative effect, and provides outlooks on further applications regarding the surface effect. This review is beneficial for designing nano-enabled photodetectors, harsh electronics, memories, sensors and transistors via surface engineering.

1. Introduction

Since the beginning of the 21st century, the scientific community has demonstrated many promising applications based on metal oxides due to their unique physical, chemical and optical properties. The distinct properties of metal oxides originate from the surface effects, including surface band bending (SBB), surface roughness, gas chemisorption, photodesorption, and surface-related defects/states.[1,2] Because metal oxide can be synthesized by a great variety of available depositing methods, complex-shaped nanostructures are achievable.[3-8] As shrinking the sizes, the increase in surface area to volume ratio (S/V) make the surface effect become more pronounced. From electrical point of view, because the charge screening length (Debye length) is in the same level (~ 100 nm) of material thickness, altering the surface states could cause a dramatic change in electric properties.[2] At the nanoscale level, the surface effect is ambiguous since it can act as either a detrimental or beneficial role depending on the application. Regarding the vulnerability of nanomaterials to the variance of surroundings, such effects are usually detrimental in device level applications. For example, a problem faced in an oxide transistor is that the interaction with ambient molecules and illumination photons could cause degradation of devices' performance. In addition, the performance of resistive switching–based devices could degrade with variation of environment conditions due to the environment-induced instability. On the other hand, facilitated by surface effects, the performance and sensitivities of the nano-enabled sensors could be greatly improved. For example, nanostructures with higher S/V ratio exhibit superior sensitivity in optical and chemical sensors comparing to their thin film counterparts.[9,10] Furthermore, surface modifications enable the electronic properties to be engineered in nanoscale.[11,12] Effective modifications could be achieved by chemical or physical approaches, helping to improve the sensitivity, detection, selectivity, and stability of the devices. Surface modifications are not only important in metal oxide-based but every class of nanoscale devices, such as organic thin-film transistors (OTFTs).[13-15] By applying the surface effect in nanoscale devices, versatile applications can be realized which pave new ways for development of high-potential technology beyond the well-established silicon-based electronics as well as optoelectronics.

In order to develop the novel application of nanostructures utilizing the surface effect, it is very important to understand how the physical properties are affected as the material dimensions are reduced. In this review, we present the surface effect on metal oxide-based nanodevices, including photodetectors, harsh electronics, resistive random access memories, gas sensors and transistors. We highlight the benefits, discuss the major constraints arising from its detrimental consequences, and provide perspective outlooks for future device applications.

2. Surface Effect in Different Types of Nanodevices

2.1. Appling the surface effect in nano-optoelectronics and eliminating the surface-induced instability for harsh electronics

Metal-oxide nanomaterials are promising in applications of photodetection and photovoltaic for their ultrahigh sensitivity and spectral selectivity. As a record, ultrahigh internal photogain up to 10^8 has been observed in ZnO nanowire (NW) device.[16] High photosensitivities are attributed to the presence of abundant deep-level states at metal oxides' surface

a Computer, Electrical and Mathematical Sciences and Engineering (CEMSE) Division, King Abdullah University of Science & Technology (KAUST), Thuwal 23955-6900, Saudi Arabia. E-mail: jrhau.he@kaust.edu.sa

combining with a gas desorption/reabsorption process. In detail, the trap states at surfaces serve as the adsorption sites for gas molecules, namely O_2, to adsorb on the metal oxide surface and capture free electrons. The absorbed molecules act as acceptors which reduce the free carrier density and deplete the surface electron states, leading to the formation of the space charge region and surfaces band bending (SBB). While illuminating by the light, the photo-generated electron-hole pairs are separated by the built-in potential formed by SBB, where the holes neutralize the O⁻ which leads to a desorption process of the oxygen. Therefore, since the holes are "trapped" by the oxygen desorption/reabsorption process, the lifetime of the electrons is greatly prolonged, leading to the ultrahigh photogain.

Taking ZnO NWs as an example, the band bending is up to 1.5 eV and a few tens of nanometers in width (1.5 eV and 43 nm measured in Air, respectively), determined by ultraviolet photoelectron spectroscopy (UPS) (Figure 1a).[2] A 100 °C heat treatment could cause a decrease of the SBB (from 1.5 eV to 0.74 eV and 43 nm to 30 nm) attributed to the removal of adsorbed oxygen molecules from the nanomaterials' surfaces. On the other hand, decoration of Au nanoparticles (NPs) can enhance the SBB to 2.3 eV and 53 nm in width due to the creation of open-circuit nano-Schottky junctions and catalytically increase the amount of the O_2 adsorbates (Figure 1b). Since the photon-electron conversion behaviours are dominated by the SBB, optoelectronic properties of metal oxide are tuneable through the engineering of this trivially thin region near the surface.[11,12] One simple way to control the optoelectronic properties is by engineering the size of the nanomaterials. For example, ZnO NW devices can be fully depleted or partially depleted, simply determining by the diameter of the NWs.[11] Decreasing the diameter of NWs from 400 to 100 nm, the response speed increases from 31 to 5 s due to the diameter-dependent SBB. To engineer the surface effect, Chen et al. have shown that by decorating the Au NPs, the sensitivities of ZnO NWs-based photodetectors can be enhanced due to the enhancement of the surface effect.[12,17] To further deplete the surfaces, Retamal et al. recently have demonstrated that n-type ZnO NWs decorated by p-type single-crystalline NiO NP decoration can produce a photogain of ~2.8 × 10⁸, which are 3 orders of magnitude higher than that of pristine ZnO NWs (Figure 1c).[18]
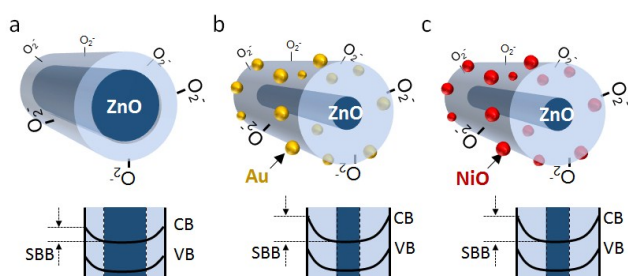
trade-off owing to the slow adsorption/desorption process.[16] This effect reduces the response speed to an unsatisfied value from several to several hundred seconds. Those faulty features limit their applications for various tasks and preclude the opportunities of metal-oxide nanodevices for real-time sensing. Some strategies have been proposed for the improvement of the reponse speed. From the electrical viewpoint, during light illumination, the generated electrons keep on accumulation, resulting in a rise of photocurrent until the equilibrium of O_2 desorption and readsorption processes. As turning off light, holes recombine quickly with electrons, while there are still a lot of electrons left in the metal oxides. It takes time for oxygen molecules to readsorb onto the surface and capture these electrons, leading to a slow recovery time. By fabricating the device with Schottky contact, photon-electron couplings within materials can be facilitated and the response speed can be improved *via* the quick regulation of the Schottky barrier height.[19, 20] The use of one-Schottky-contact geometry reported by Zhou et al. demonstrates that both the sensitivity of a ZnO NW photodetector can be greatly promoted with an improved response time of 0.6 s.[16] Multiple junctions can be formed by introducing a network scheme, which is an effective approach to improve recovery speed. For example, Chen et al. have shown that by fabricating the devices in a network manner, the response speed can be improved by 2 order compared to the single nanobelt devices (Figure 2a and 2b).[21,22] To maximize the Schottky contact, modification through a nanostructure design, for example, core-shell geometries or decoration of metal particles provides viable routes for the same purpose. For example, Hsu et al. reported an integration of multi-walled carbon nanotubes (MWCNT) and TiO_2 shells to form radial Schottky barriers in a core-shell fashion (Figure 2c).[23] By this core-shell design, radial Schottky barriers between carbon nanotube cores and TiO_2 shells can effectively regulate electron transport, leading to ultrahigh photogain (1.4×10^4) and the ultrashort response/recovery times (4.3/10.2 ms) (Figure 2b). Additionally, radial Schottky junction and defect band absorption broaden the detection range (UV–visible) (Figure 2d).

Fig. 1 The schematic of surface band bending for (a) oxygen-adsorbed NWs, (b) Au-decorated NWs and (c) NiO-decorated NWs.

However, as a side effect, high photogain metal-oxide devices normally suffer from the detrimental responsivity-speed
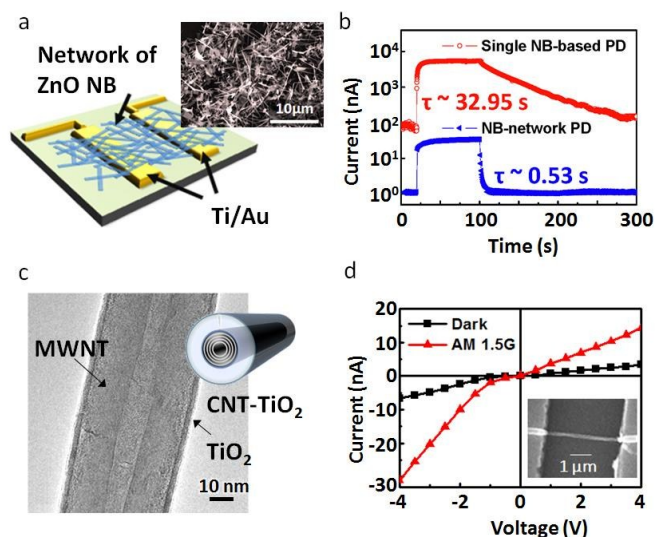
Fig. 2 (a) Schematic of the ZnO NB networks photodetector. The inset is the top-view SEM image of the ZnO NBs on the prefabricated Ti/Au electrodes. (b) Comparison of the time-resolved photocurrents of the ZnO NB networks and a single ZnO NB under the UV illumination. (c) A TEM image of a TiO_2-coated MWNT core-shell NW. (d) *I-V* characteristics of the TiO_2 coated MWNT photodetector in dark and under AM 1.5G illumination. The inset is the SEM image of the devices. The images are replotted from references 21, 22, and 23. (Copyright of American Chemical Society.)

In the view of optics, performance of nano-optoelectronics can be enhanced by employing nanophotonic technique which supports a sophisticated management of light. For example, the technique of photon management using nanostructures has been widely used to boost the efficiency of photodetectors, light emitting diode, and solar cells.[7,24-28] Considering the surface effect of metal oxide materials, light absorption near the surface is much more efficient than the absorption in deeper region of the bulk. As such, a resonant mode capable of near-surface light concentration is preferred, which can prevent intrinsic optical losses. Recently, we demonstrate a resonant scheme that can facilitate the light-matter coupling by exciting resonance within multi-nanoshelled ZnO structures.[29] Due to the resonance-assisted effect by the concentric shells, the nanoshells can absorb > 90% of UV light as compared with an equivalent volume of bulk counterparts. The nanoshell devices show enhanced optoelectronic performance and omnidirectional detectability both for incident angle and light polarizations. The general design principles behind the multishelled hollow ZnO nanoshells pave a new way to improve the performance of sophisticated nanophotonic photodetectors.

By introducing high-crystallinity metal oxide materials, one can eliminate the surface effect as so to improve the stabilities of photodetectors for uses in extreme conditions. For example, Wei et al. demonstrate a fully-transparent photodetectors based on β-Ga_2O_3, which is capable of being operated under high temperature (700 K) and high voltage (200 V) conditions without breaking down.[30] He shows that under different oxygen concentration (i.e., vacuum (10^{-5} Torr), air, and pure oxygen), the performance of metal oxide photodetectors does not change significantly, indicating that the photocurrent is not dominated by surface effect due to the superior crystal quality. This work

demonstrates an effective way to fabricate photodetectors for uses in extreme operation conditions.

Another field related to surface effect is the harsh electronic which is an emerging field aiming to promote device capability in strict environment conditions. Specific applications including oil, gas, geothermal, aircraft/automotive engines aerospace/military, and industrial uses, require this type of devices for operating in extremes of radiation, pressure, temperature, shock, and chemically corrosive liquids/gases environments. To develop optoelectronics for harsh environments, we recently show that the photodetectors made by AlN can work at temperature up to 300 °C with radiation tolerance up to 10^{13} cm^2 of 2-MeV proton fluences because of its superior thermal stability and high radiation resistance.[31] To further improve the performance in harsh environments, by introducing the multiple quantum wells (MQWs) into solar cells the efficiency can be enhanced by 0.52%/°C and exhibit superior radiation robustness (lifetime 430 years under solar storm proton irradiation) for their strong atomic bonding direct-bandgap characteristics. This study also provides valuable routes for future developments in self-powered harsh electronics.

2.2. Surface effect in metal-oxide memory devices and their passivation

Resistive random access memory (ReRAM), one of the potential candidates in next-generation memory, has attracted intensive attention owing to its nonvolatility, high writing/reading speed, high density, and low power consumption.[32-35] ReRAM is promising for the simplicity of device structure, ease of device fabrication and comparability to be fabricated on different types of substrate. An interesting example is the new type ReRAM recently demonstrated on the "paper" substrate, which is constructed by a simple metal-insulator-conductor structure (Ag/TiO_2/C) using all-printing techniques (Figure 3a).[33] This work shows that the ReRAM is readily fabricated on any flexible substrates and labeled on electronics or living objects for multifunctional, wearable, on-skin, and biocompatible applications (Figure 3b). Recently, a cellulose-based ReRAM has demonstrated ultra-high flexibility capable being bent down to the radius of 350 μm, which is the smallest value compared to any existing flexible ReRAM.[35] Due to the simplicity of structure, an ultra-high memory density based on vertical-resistive random access memory is achievable.[36] Durán Retamal et al. have demonstrate that ultrathin sidewalls of C54-$TiSi_2$ nanoscale electrodes can confine and stabilize the random nature of the resistive switching process by acting as the seeds for conducting nanofilaments growth. As a result, with C54-$TiSi_2$ as horizontal electrodes, a 3D-stacking memory can be achieved (Figure 3c and 3d). Another advantage of the ReRAM is the low power consumption. Very recently, Kang et al. have shown that the nonvolatile memory made by BMO exhibits excellent resistive switching performance and can be operated with ultralow power consumption (i.e., 3.8 and 20 fJ for set and reset process).[37] The lower consumption power reults from the

conducting nanofilement formation energy, where the nanofilements are only 10 nm in diameter and are seperate by 20–30 nm in spacing, determined by transimission electron microscopy (TEM). Formation of nanofilement in ReRAM devices has recently been observed by in-situ TEM techniques and conductive atomic force microscopy, revealing the microscopic origin behind resistive switching and offering guidance for the design of novel ionic devices.[38,39]
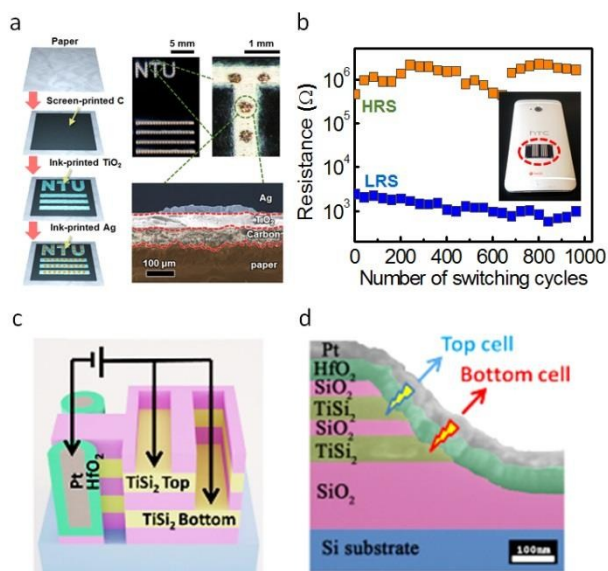
Fig. 3 (a) Schematic diagram of the fabrication process for the resistive paper memory device. Photograph of the device, where the alphabetical letters and the line arrays composed of Ag and TiO$_2$ demonstrate the degree of freedom for the inkjet-printed patterns. (b) The switching characteristics of a paper memory label tagged on a smart phone. (c) Schematic of the 3D double-layer vertical ReRAM. (d) The cross-sectional SEM images of 3D vertical ReRAM devices. Copyright of American Chemical Society and AIP Publishing LLC.

Using metal oxide materials as active layers in ReRAM are ideal due to their highly tuneable electric resistance and solid electrolyte characteristics.[40-47] Metal oxide material systems, including perovskite-type oxides, ferroelectric oxides, binary transition metal oxides and complex metal oxide, have been demonstrated to be applicable in resistive switching.[48-50] However, the surface effect, an intrinsic nature of metal oxide materials, is detrimental to device applications because of the induced electrical instability.[51-54] Because the resistive switching mechanism is associated with the formation/rupture of the conductive nanofilaments near the oxide-electrode interface, the switching characteristic could be influenced by the chemisorbed O$_2$ molecules at the surfaces. The evidence is that the interaction between chemisorbed oxygen and oxygen vacancies in oxides dominates the switching features of ZnO-based ReRAM.[52] The absorbed oxygen causes an increase of resistance in high resistance state (HRS). Meanwhile, surface effect becomes more and more pronounced during operation due to Joule heating as the voltage is continuously applied. This leads to the fact that the resistive switching performances of oxide memory devices, including switching yield and resistance value fluctuation, are sensitive to the ambiences.

Sealing and packaging are often applied to memory devices to temporally deal with varied environmental conditions. However, to achieve long-term reliability, it is necessary to modify the material as inert as possible, and thus finding approaches to achieve stable switching is in particular demand. One way to reduce the surface susceptibility is through atomic doping. For example, doping nitrogen into ZnO by employing an atomic layer deposition (ALD) technique has been proposed to improve the stability and reliability of ZnO resistive memory.[53] The mechanism is that the doped nitrogen can compensate the native defects and reduce oxygen molecule chemisorption, which suppresses the surface effects on the memory switching behaviours. Consequently, the memory devices exhibit better immunity against ambient conditions.

It has shown that even in mild ambient condition changes, the performance metal oxide memory can be greatly affected. In certain harsh conditions, the degradation of the memory performance becomes worse because some metal oxides are extremely sensitive to corrosive atmospheric exposure and surface contamination associated with corrosion attack. As an example, ZnO is chemically unstable in acetic conditions.[4-57] The formic acid molecules can weaken the Zn–O bonds, leading to Zn atom dissolution processes, which spread throughout the material until the device failure occurs. Therefore, even though ZnO-based electronic and optoelectronic devices exhibit fascinating performances, severe chemically instability would hinder their practical uses. The surface/interface modification by CF$_4$ plasma treatment improves the resistive switching characteristics of the ZnO thin films. [54] This treatment not only prolongs the device endurance, but also stabilizes the switching parameters, including set voltage (V_{set}), reset voltage (V_{reset}) and reset current. Moreover, the surface modification with fluorine allows the ZnO ReRAM to withstand severe corrosive conditions (Figure 4a and 4b). Improved ReRAM characteristics, high inertness to surface effect, and high durability in acetic environment are due to surface passivation (saturating the dangling bonds and diminishing the oxygen vacancies) and strong Zn-F bonding (preventing the Zn atoms from dissolution) via the fluorine incorporation. The ability for the devices to operate in various ambiences, including chemically harsh conditions, with long term durability and reliability will play an important role in the successful emergence of resistive memory based on ZnO.
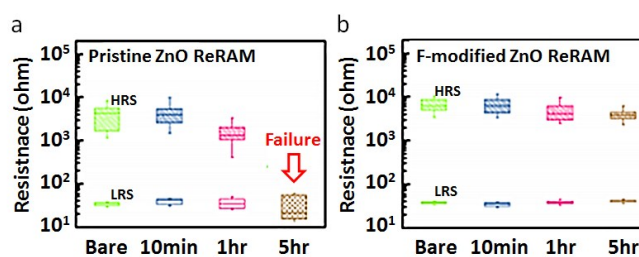
Fig. 4 Box and whisker plots for the atmosphere-dependent resistance in HRS and LRS of (a) pristine ZnO. (b) F-modified ZnO devices. The ambience of vacuum, nitrogen, air, and oxygen are denoted as Vac., N$_2$, Air, and O$_2$, respectively. Copyright 2014, Nature Publishing Group.

A new approach to protect the memory from environmental interference is to apply two-dimensional (2D) passivation using atomically thin 2D nanomaterials. 2D materials are the thinnest functional nanomaterials regarded as attractive substitutes to many traditional materials.[58-66] Recently, Yang *et al.* reported that by introducing graphene electrodes as a passivation layer the surface effect in memory can be suppressed via eliminating the detrimental effect from the chemisorbed O_2 molecules.[44] As tested in different atmosphere, ZnO with graphene as passivation layer shows lower variation in switching yield (yield ranging from 66.7% to 75.0%) as compared to that of pristine ZnO (yield ranging from 41.7% to 66.7%) (Figure 5a and 5b). In addition, due to low sheet resistance and high optical transparency of graphene, ZnO memory devices exhibits not only stable resistive switching characteristics but also excellent transparency (less than 2% absorptance by graphene) (Figure 5c).
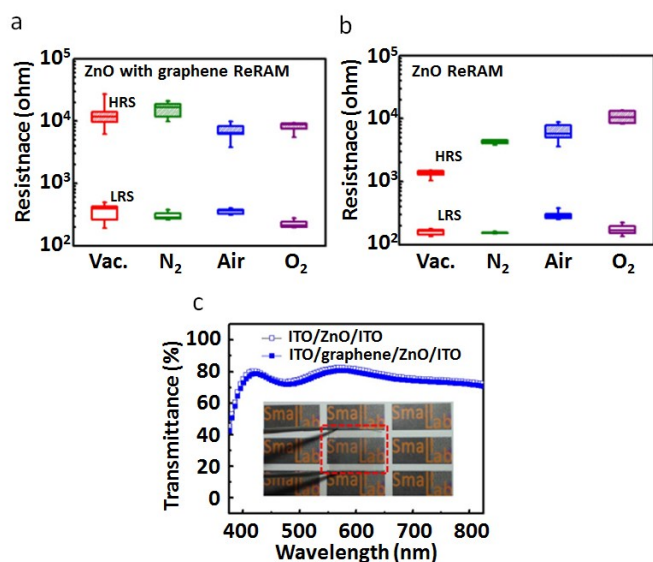
Fig. 5 Plots for the atmosphere-dependent resistance changes in HRS and LRS of the memory device (a) with and (b) without graphene electrodes. (c) The transmittance of ITO/ZnO/ITO/glass (open squares) and ITO/graphene/ZnO/ITO/glass (solid squares) devices within the ITO/graphene/ZnO/ITO transparent ReAM device. The background can be observed through the device. Copyright 2014, IEEE.

Although the surface effects are mostly unfavourable to memory devices, a well control of the effects can help to promote the performance of memory. Recently, Durán *et al.* show that the photoelectrical and resistive switching properties of ZnO ReRAM can be tuneable by a treatment of ultraviolet (UV) illumination. Based on the regulation of oxygen photodesorption and readsorption by UV illumination, the treatment can significantly reduce the variations of resistance in high resistance state, set voltage and reset voltage by 58%, 33%, and 25%, respectively.[67] This finding gives physical insight into designing a stable resistive memory device in the future.

2.3. Applying the surface effect in gas sensors

Form the photodetectors to memory devices, it has shown that the electronic and optoelectronic properties of metal oxide-based devices can be significantly influenced by engineering the electronic states at surfaces.[68] The mechanism is due to the gas adsorption which tunes the electronic band bending at the surface, and apparently, gases in different classes can produce various effects. Based on this mechanism, gas sensors are achievable through a proper design of the metal oxide devices.[69,71] There is a strong interest in the development of lightweight gas sensors capable of sensing chemicals in parts-per million (ppm) range with low-power consumption. It has demonstrated that metal oxide-based sensors are capable of detecting gases, such as NO_2,[72] NH_3,[73] NH_4,[74] CO,[75] H_2,[?] H_2O,[76] O_3,[77] H_2S,[78] and C_2H_5OH, with high sensitivity.[79] The fundamental mechanism of the gas sensor is to change the conductivity *via* the electron trapping and releasing on the surface. In principle, as gas molecules are adsorbed on surface, charge transfer occurs which modifies the carrier concentration, resulting in a change of conductivity. For example, with NO_2 or O_2 adsorption, the molecules tend to capture free electrons on the surface, forming a low-conductivity depletion layer near surfaces and decrease the conductivity of ZnO devices.[80-83] On the other hand, reductive gases, such as ethanol, H_2, CO, and H_2S, react with the charged oxygen molecules on surfaces, and thus free electron concentration is increased due to oxygen desorption, leading to an increase of conductivity.[84-88]

Since the gas sensing mechanism relies on the surface effects, the sensitivity of the sensors can be improved by the surface modification which could enhance the surface effect. For example, the sensitivity of ZnO to H_2 sensing can be improved by Pd clusters decoration on the device surface. The addition of Pd catalytically helps the dissociation of H_2 into atomic hydrogen, increasing the sensitivity of the sensor device. This sensor can detect hydrogen with concentrations down to 10 ppm, whereas there is no response to O_2. The same concept also works on ZnO NWs gas sensor, whose H_2 detection sensitivity can be promoted by Pt coating.[89] Electrode selection is another way to improve the gas sensor. For example, using Pt interdigitating electrodes, a metal oxide sensor with good ethanol sensitivity and fast response at 300°C has been demonstrated.[90] Introducing heterojunctions to create hybrid nanomaterials is another strategy to improve the sensitivity. Ho *et al.* has reported that the plasma-polymerized acrylonitrile/ZnO sensor offers significant advantages over conventional ZnO gas sensors.[70] The minimum sensitivity can achieve 16.6 ppm, which is decent for gas sensors, especially combined with a low working temperature (Figure 6a). The results show that under UV light illumination oxygen sensing of PP-AN/ZnO NBs can be enhanced significantly because the effects of oxygen desorption/adsorption of the polymer on the electron depletion region of the ZnO is pronounced under UV light (Figure 6b and 6c). The sensing behaviours of the bilayered nanomaterial demonstrated performance in terms of sensitivity and working temperature due to the adsorption nature of the polymer.
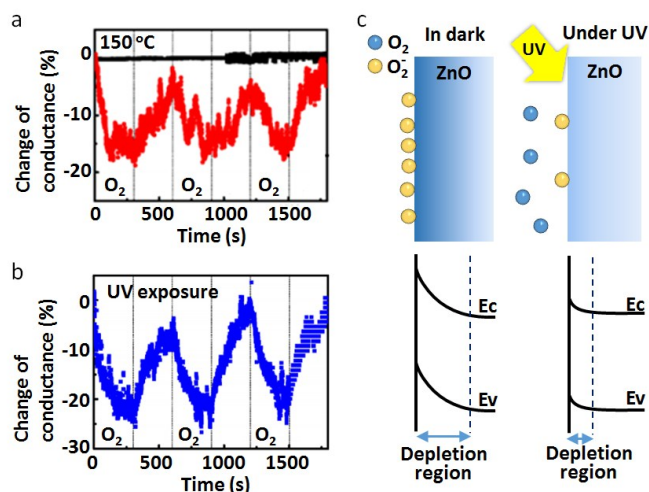
Fig. 6 (a) Gas-sensing properties of PP-AN/ZnO nanobelt under the fixed bias at 1 V in response to oxygen of 150 ppm concentration in the dark at a working temperature of 125 °C (black) and 150 °C (red). (b) Operation with a working temperature of 150 °C under 365 nm UV light illumination. (c) In the illuminated state, photogenerated holes recombine with trapped electrons at the surface, desorbing electron-trapping oxygen molecules, such as O$^-$ and O^{2-}. The depletion region reduces and the ZnO nanobelt conductivity increases by modifying the surface potential. The figures are replotted from reference 70. Copyright of IOP Publishing.

2.4. Surface effect in metal oxide transistors

Another fundamental research area of metal oxide are thin film transistors (TFT)[91,92] and NW field effect transistors (FET).[93,94] The electrical tunability of metal oxide from insulator to metal, owing to the large difference in electronegativity between the heavy metal cations and oxygen atoms, has led to the development of high performance transistors with high field-effect mobility (μ), low off current (I_{off}), steep subthreshold swings (SS) slope and large on-off current ratio (I_{on}/I_{off}).[95,96] Many studies have shown that oxide TFTs are the best candidates as gate driver and pixel switching devices in the active-matrix of liquid crystal and organic light emitting diode for next generation displays.[92] However, a common problem faced in oxide TFTs is the adverse environmental effect that results from the interaction with ambient molecules and illumination photons on the metal oxide surface.[97] The adsorption/desorption dynamics of molecules and photons onto the exposed channel surface significantly affect performance by reducing μ, increasing I_{off}, lowering SS, reducing I_{on}/I_{off} and shifting threshold voltage (V_{th}) and thus becoming a critical problem for stability (Figure 7a).

The effect of the environmental humidity on metal oxide is of special importance because oxygen and water molecules in the ambient atmosphere are known to induce the degradation of bias-stressed transistors and play an important role in carrier transport. It has been confirmed that adsorbed oxygen on the ZnO surface can capture an electron from the conduction band and that the resulting oxygen species can exist in various forms such as O$_2^-$, O$^-$, or O^{2-}, as described by the following chemical reaction $O_{2(gas)} + e^- \rightarrow O_{2\;(ads)}^-$.[98,99] As a result of charge transfer, a depletion layer is formed beneath the Zn-based oxide surface, leading to reduced carrier concentration that might end up in enhancement mode transistors.[100] The surface effect manifests itself as a continuous increase in V_{th} when the gate bias is kept constant over time (Figure 7b). Assuming an exponential distribution of trap states at room temperature T, the V_{th} shift (ΔV_{th}) at infinite stress time is equal to the applied gate bias required to compensate the electric field created by trapped charges before an accumulation layer is formed, yielding a stretched exponential decay for V_{th} with time $\Delta V_{th} = V_0(1-exp(-(t/\tau)^\beta)))$, where τ is a characteristic time constant thermally activated, β is the dispersion parameter equal to T/T_0, and $V_0 = V_G - V_{th0}$, where V_{th0} is the V_{th} at the start of the experiment.[101] The ΔV_{th} is also remarkably more pronounced with the variation of oxygen partial pressure and can be modeled by the Freundlich adsorption model which states that V_{th0} at oxygen pressure P can be expressed as $ln(V_{th0}^P)=constant+(1/n)ln(P)$, where n is constant.[92]
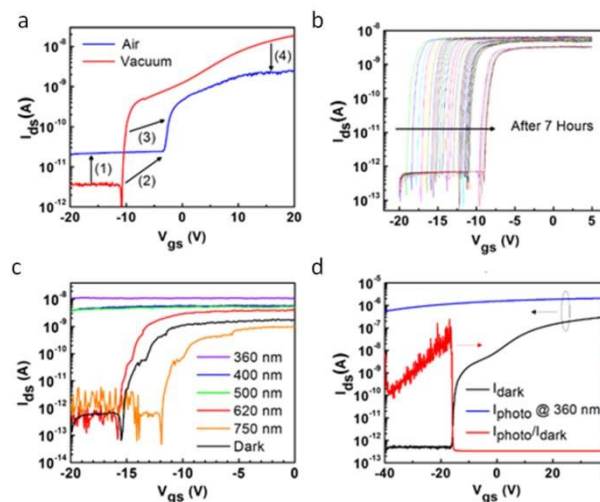
Fig. 7 (a) I_{ds}-V_{gs} curves at V_{ds} = 1 V of ZnO NW-FET. (a) Degradation from vacuum to air conditions. The numbers indicate: (1) I_{off} increase, (2) positive ΔV_{th}, (3) SS reduction, and (4) I_{on} decrease. (b) Repeated measurements over time during hours with continuous positive ΔV_{th}. (c) Wavelengths illumination dependence indicating surface illumination interaction effect. (d) Dark current (I_{dark}) and photocurrent (I_{photo}) at 360 nm illumination. Right axis is photocurrent to dark current ratio, indicating maximum ratio occurs below the SS slope. Copyright of AIP Publishing LLC.

Because of the wide band gap of certain metal oxides, transparent transistors can be integrated into displays.[102] However, the surface illumination interaction effect can lead to operation sensitive to visible light irradiation.[97] Figure 7c shows the variation of transfer characteristic under different wavelength illumination. In contrast, regarding the surface interaction with UV illumination as explained in the PD section, there is an advantage in using photo-transistors rather than two-terminal photodetectors due to the photo-response properties that can be modulated by gate bias.[103,104] When the photo-transistor is in the on-state bias the photocurrent is dominated by the photovoltaic effect and the photo-generation is minimum, because at this gate bias the dark current also increases. Whereas, in the off-state, photoconductivity effect is

significant for the transistor, and the photo-generation is maximum, because at this gate bias the carrier injection and thermal generation have the smallest contribution to photo-generation and in turn photo-generated current has the highest contribution just below the SS slope (Figure 7d). However, UV illumination causes significant negative ΔV_{th}, and the recovery upon turn off UV illumination is slow, leading to problems during normal device operation. The V_{th} instability caused by UV illumination is attributed to positive charge trapping, while the slow recovery involves the recombination of oxygen vacancies, free electrons, and oxygen atoms.[103] The energy of UV photons would help the oxygen atoms diffuse into an interstitial site. After switching off the UV illumination, the interstitial oxygen atoms require relatively high energies to diffuse back to the lattice site. This is because the diffusing oxygen atoms must overcome the potential barrier due to the surrounding ions. Hence, it takes some time for the system to return to the initial pre-illumination state at room temperature.[105]
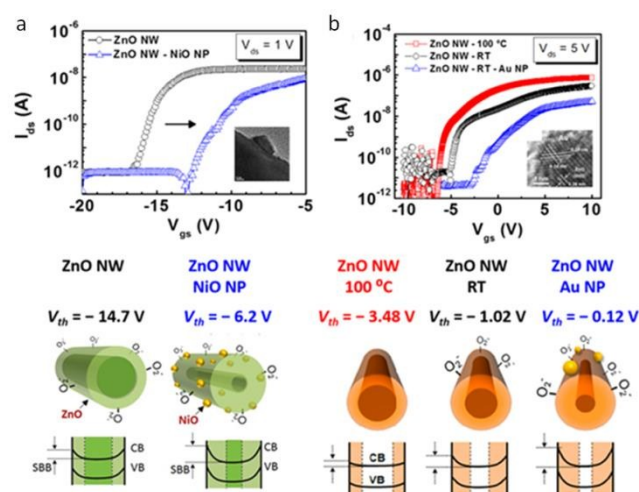
Fig. 8 (a) Positive shift of the I_{ds}-V_{gs} curve at V_{ds} = 1 V of ZnO NW-FET after NiO NP decoration, showing a positive ΔV_{th} from -14.7 V to -6.2 V. The inset shows a HRTEM image of a NiO NP decorating ZnO NW. Schematics of the SBB caused by oxygen chemisorption for pristine NWs and NWs with *pn* nano-junctions.[15] (b) Positive and negative shift of the I_{ds}-V_{gs} curve at V_{ds} = 5 V of ZnO NW at room temperature (RT) when heated at 100 °C, and decorated with Au NP respectively, showing a negative and positive ΔV_{th} from -1.02 V to -3.48 V and from -1.02 V to -0.12 V, respectively. The inset shows a HRTEM image of a Au NP decorating ZnO NW. Schematics of the SBB caused by oxygen desorption at 100 °C, oxygen chemisorption for pristine NWs at RT, and NWs with Schottky nano-junctions *via* Au NPs.[2] (Copyright of American Chemical Society.)

Furthermore, nanoparticle decoration provides an alternative route to manipulate intrinsic properties of metal oxides *via* SBB modulation. Positive ΔV_{th} has been observed when decorating the metal oxide surface with either metallic or semiconducting NPs. For example, Au NPs[2] and *p*-NiO NPs[18] forming Schottky and *pn* nano-junctions on *n*-ZnO, respectively, enhance the depletion region by favouring oxygen adsorption and thus resulting in positive ΔV_{th}, as it is shown in Fig. 8a and 8b. In contrast, in order to counteract the positive ΔV_{th} due to oxygen adsorption, thermal treatment at 100 °C can serve to prompt oxygen desorption and thus induce negative ΔV_{th} to recover the

depletion region, as it is shown in Fig. 8b.[92] These results highlight the versatility in tuning the depletion region of metal oxides via surface treatment, and hence its FET properties boosting the optical, and chemical sensing capabilities.

3. Conclusions and Outlook

3.1. Examining the surface effects in electronics

Surface effects are pronounced in nanoscale devices and are proved to have huge impact on the device performance. These effects could cause either a detrimental or beneficial impact based on the application of the devices. Any nanodevice subjected to surface effect must be able to be fabricated and function stably before commercialized. To control the effect, intrinsic capabilities and limiting factors, such as the cause of surface effect and environment interaction, should be well understood in order to engineer the effect. In this review, we have shown that the surface effect can be investigated electrically and optically by different types of measurements such as field-effect device measurement and UPS. However, challenges to comprehensively control the properties and maintain reliability still remain. After understanding the underlying mechanisms, one can guarantee the required level of device stability and reliability under various external conditions.

3.2. Application of surface effect in devices

For metal oxide optoelectronics, the surface effect contributes to high sensitivity but reduces the response speed. Finding a solution to compensate the trade-off between sensitivity and speed is crucial for pushing the metal oxide optoelectronics into real applications. In this review, we have shown different strategies, including surface modification and geometry design, to improve the response speed and at the same time keep the high sensitivity. In addition, since depleted region is only a few tens of nanometers near the surface, most light is penetrating and absorbed in bulk, wasted by fast recombination. To increase effective absorption, we proposed a resonant model capable of near-surface concentration which is preferred for metal oxide photodetectors. For memory devices, the surface effect is usually detrimental to device applications because of the induced instability. We have examined several environmental factors that could affect the performance of the ReRAM, including the gas absorption and corrosive sources. We show that using atomic doping, surface modification and 2D material passivation, it is possible to stabilize the performance of ReRAM from surface effect. Since the gas adsorption is the main cause of surface effect, gas sensing is workable and promising for metal oxide devices. We have shown that by combining nanomaterials in different classes, desired device performance can be achieved and the sensitivity can be improved. The same concepts are applicable in metal oxide transistors. We have shown that by proper treatment of UV light, surface effect can be controlled and the performance of metal oxide can be promoted.

References

1. W. Park, G. Jo, W. K. Hong, J. Yoon, M. Choe, S. Lee, Y. Ji, G. Kim, Y. H. Kahng, K. Lee, D. Wang and T. Lee, *Nanotechnology*, 2011, **22**, 205204.
2. C. Y. Chen, J. R. D. Retamal, I. W. Wu, D. H. Lien, M. W. Chen, Y. Ding, Y. L. Chueh, C. I. Wu and J. H. He, *ACS Nano*, 2012, **6**, 9366-9372.
3. Z. W. Pan, Z. R. Dai and Z. L. Wang, *Science*, 2001, **291**, 1947-1949.
4. Z. L. Wang, *J. Phys. Condens. Matter*, 2004, **16**, R829-R858.
5. Z. H. Dong, X. Y. Lai, J. E. Halpert, N. L. Yang, L. X. Yi, J. Zhai, D. Wang, Z. Y. Tang and L. Jiang, *Adv. Mater.*, 2012, **24**, 1046-1049.
6. Z. Fan and J. G. Lu, *J. Nanosci. Nanotechnol.*, 2005, **5**, 1561-1573.
7. Y. H. Hsiao, C. Y. Chen, L. C. Huang, G. J. Lin, D. H. Lien, J. J. Huang and J. H. He, *Nanoscale*, 2014, **6**, 2624-2628.
8. H. Ko, Z. Zhang, K. Takei and A. Javey, *Nanotechnology*, 2010, **21**, 295305.
9. E. Comini, G. Faglia, G. Sberveglieri, Z. Pan and Z. L. Wang, *Appl. Phys. Lett.*, 2002, **81**, 1869-1871.
10. M. Law, H. Kind, B. Messer, F. Kim and P. Yang, *Angew. Chem. Int. Ed.*, 2002, **114**, 2511-2514.
11. M. W. Chen, J. R. D. Retamal, C. Y. Chen and J. H. He, *IEEE Trans. Electron Dev.*, 2012, **33**, 411-413.
12. M. W. Chen, C. Y. Chen, D. H. Lien, Y. Ding and J. H. He, *Opt. Express*, 2010, **18**, 14836-14841.
13. P. Lin and F.Yan, *Adv. Mater.* 2012, **24**, 34–51.
14. C. D. Dimitrakopoulos and P. R. L. Malenfant, *Adv. Mater.* 2002, **14**, 99-117.
15. S. C. Lima, S. H. Kima, J. H. Leea, M. K. Kima, D. J. Kimb and T. Zyunga, *Synt. Met.*, **148**, 75–79.
16. C. Soci, A. Zhang, B. Xiang, S. A. Dayeh, D. P. R. Aplin, J. Park, X. Y. Bao, Y. H. Lo and D. Wang, *Nano Lett*, 2007, **7**, 1003-1009.
17. K. W. Liu, M. Sakurai, M. Y. Liao and M. Aono, *J. Phys. Chem. C*, 2010, **114**, 19835-19839.
18. J. R. D. Retamal, C. Y. Chen, D. H. Lien, M. R. S. Huang, C. A. Lin, C. P. Liu and J. H. He, *ACS Photonics*, 2014, **1**, 354-359.
19. J. Zhou, Y. D. Gu, Y. F. Hu, W. J. Mai, P. H. Yeh, G. Bao, A. K. Sood, D. L. Polla and Z. L. Wang, *Appl. Phys. Lett.*, 2009, **94**, 191103.
20. Q. Yang, X. Guo, W. H. Wang, Y. Zhang, S. Xu, D. H. Lien and Z. L. Wang, *ACS Nano*, 2010, **4**, 6285-6291.
21. C. Y. Chen, M. W. Chen, C. Y. Hsu, D. H. Lien, M. J. Chen and J. H. He, *IEEE J. Sel. Top. Quantum Electron.*, 2012, **18**, 1807-1811.
22. C. Y. Yan, N. Singh, H. Cai, C. L. Gan and P. S. Lee, *Acs Appl Mater Inter*, 2010, **2**, 1794-1797.
23. C. Y. Hsu, D. H. Lien, S. Y. Lu, C. Y. Chen, C. F. Kang, Y. L. Chueh, W. K. Hsu and J. H. He, *ACS Nano*, 2012, **6**, 6687-6692.
24. M. L. Brongersma, Y. Cui and S. H. Fan, *Nat. Mater.*, 2014, **13**, 451-460.
25. S. F. Leung, Q. P. Zhang, F. Xiu, D. L. Yu, J. C. Ho, D. D. Li and Z. Y. Fan, *J. Phys. Chem. Lett.*, 2014, **5**, 1479-1495.
26. H. P. Wang, D. H. Lien, M. L. Tsai, C. A. Lin, H. C. Chang, K. Y. Lai and J. H. He, *J. Mater. Chem. C*, 2014, **2**, 3144-3171.
27. C. H. Ho, D. H. Lien, H. C. Chang, C. A. Lin, C. F. Kang, M. K. Hsing, K. Y. Lai and J. H. He, *Nanoscale*, 2012, **4**, 7346-7349.
28. Y. Yao, J. Yao, V. K. Narasimhan, Z. C. Ruan, C. Xie, S. H. Fan and Y. Cui, *Nat. Commun.*, 2012, **3**, 664.
29. D. H. Lien, Z. Dong, J. R. Duran Retamal, H. P. Wang, T. C. Wei, S. C. Lee, D. Wang, J. H. He, Y. Cui, *Nat. Commun.*, in press.
30. D. S. Tsai, C. A. Lin, W. C. Lien, H. C. Chang, Y. L. Wang and J. H. He, *Acs Nano*, 2011, **5**, 7748-7753.
31. D. H. Lien, Y. H. Hsiao, S. G. Yang, M. L. Tsai, T. C. Wei, S. C. Lee, and J. H. He, *Nano Energy*, 2015, **11**, 104-109.
32. G. I. Meijer, *Science*, 2008, **319**, 1625-1626.
33. D. H. Lien, Z. K. Kao, T. H. Huang, Y. C. Liao, S. C. Lee and J. H. He, *ACS Nano*, 2014, **8**, 7613-7619.
34. R. Waser and M.Aono, *Nat. Mater.*, 2007, **6**, 833–840.
35. K. Nagashima, , H. Koga, , U. Celano, , F. Zhuge, , M. Kanai, , S. Rahong, G. Meng, Y. He, J. D. Boeck, M. Jurczak, W. Vandervorst, T. Kitaoka, M. Nogi and T. Yanagida. *Sci. Rep.*, 2014, **4**, 5532.
36. J. R. D. Retamal, C. F. Kang, P. K. Yang, C. P. Lee, D. H. Lien, C. H. Ho and J. H. He, *Appl. Phys. Lett.*, 2014, **105**, 182101.
37. C. F. Kang, W. C. Kuo, W. Z. Bao, C. H. Ho, C. W. Huang, W. W. Wu, Y. H. Chu, J. Y. Juang, S. H. Tseng, L. B. Hu, and J. H. He, *Nano energy*, 2015, **13**, 283–290 .
38. Y. Yang, P. Gao, L. Li, X. Pan, S. Tappertzhofen, S. Choi, R. Waser, I. Valov and W. D. Lu, *Nat. Comm.*, 2014, **5**, 4232.
39. U. Celano, L. Goux, A. Belmonte, K. Opsomer, A. Franquet, A. Schulze, C. Detavernier, O. Richard, H. Bender, M. Jurczak, W. Vandervorst, *Nano Lett.*, 2014, **14**, 2401–2406.
40. Y. T. Huang, S. Y. Yu, C. L. Hsin, C. W. Huang, C. F. Kang, F. H. Chu, J. Y. Chen, J. C. Hu, L. T. Chen, J. H. He and W. W. Wu, *Analyt. Chim.*, 2013, **85**, 3955-3960.
41. Y. C. Lai, F. C. Hsu, J. Y. Chen, J. H. He, T. C. Chang, Y. P. Hsieh, T. Y. Lin, Y. J. Yang and Y. F. Chen, *Adv. Mater.*, 2013, **25**, 2733-2739.
42. C. H. Huang, J. S. Huang, S. M. Lin, W. Y. Chang, J. H. He, Y. L. Chueh, *ACS Nano*, 2012, **6**, 8407-8414.
43. A. Sawa, *Mater Today*, 2008, **11**, 28–36.
44. S. L. Li, J. Li, Y. Zhang, D. N. Zhengand, K. Tsukagoshi, *Appl. Phys. A Mater. Sci. Process.*, 2011, **103**, 21–26.
45. W. Shen, R. Dittmann, R Waser, *J. Appl. Phys.*, 2010, **107**, 094506.
46. J. A. Rodriguez, J. C. Hanson, A. I. Frenkel, J. Y. Kim, and M. Pe´rez *J. Am. Chem. Soc.*, 2002, **124**, 346–354.
47. S. Wang, M. Awano, K. Maeda, *J. Electrochem. Soc.*, 2003, **150**, D209–D214.
48. D. H. Kwon, K. M. Kim, J. H. Jang, J. M. Jeon, M. H. Lee, G. H. Kim, X. S. Li, G. S. Park, B. Lee, S. Han, M. Kim, and C. S. Hwang, *Nat. Nanotechnol.*, 2010, **5**, 148–153.
49. G. H. Kim, J. H. Lee, J. Y. Seok, S. J. Song, J. H. Yoon, K. J. Yoon, M. H. Lee, K. M. Kim, H. D. Lee, S. W. Ryu, T. J. Park, and C. S. Hwang, *Appl. Phys. Lett.*, 2011, **98**, 262901.
50. H. W. Huang, C. F. Kang, F. I. Lai, J. H. He, S. J. Lin, Y. L. Chueh, *Nanoscale Res. Lett.*, 2013, **8**, 483.
51. P. K. Yang, W. Y. Chang, P. Y. Teng, S. F. Jeng, S. J. Lin, P. W. Chiu, and J. H. He, Proc. IEEE, 2013, **101**, 1732–1739.
52. J. J. Ke, Z. J. Liu, C. F. Kang, S. J. Lin, and J. H. He, *Appl. Phys. Lett.*, 2011, **99**, 192106.
53. T. H. Huang, W. Y. Chang, J. F. Chien, C. F. Kang, P. K. Yang, M. J. Chen, and J. H. He, *J. Mater. Chem. C*, 2013, **1**, 7593-7597.
54. T. H. Huang, P. K. Yang, D. H. Lien, C. F. Kang, M. L. Tsai, Y. L. Chueh and J. H. He, *Sci. Rep.*, 2014, **4**, 4402.
55. J. Zhou, N. Xu, and Z. L. Wang, *Adv. Mater.*, 2006, **18**, 2432–2435.
56. F. J. Pern, R. Noufi, B. To, C. DeHart, X. Li, and S. H. Glick, *Proc. SPIE*, 2008, 70480.
57. T. Minami, S. Takata, H. Sato, and H.Sonohara, *J. Vac. Sci. & Technol. A*, 1995, **13**, 1095–1099.
58. M. Osada and T. Sasaki, *Adv. Mater.*, 2012, **24**, 210–228.
59. Y. Shi, C. Hamsen, X. Jia, K. K. Kim, A. Reina, M. Hofmann, A. L. Hsu, K. Zhang, H. Li, Z. Y. Juang, M. S. Dresselhaus, L. J. Li, and J. Kong, *Nano Lett.*, 2010, **13**, 4134–4139
60. B. Alem´an, W. Regan, S. Aloni, V. Altoe, N. Alem, C. Girit, B. Geng, L. Maserati, M. Crommie, F. Wang, and A. Zettl, *ACS Nano*, 2010, **4**, 4762–4768.
61. D. H. Lien, J. S. Kang, M. Amani, K. Chen, M. Tosun, H. P. Wang, T. Roy, M. Eggleston, M. Wu, S. C. Lee, J. H. He and A. Javey, *Nano Letters* 2015, **15**, 1356.
62. Y. Shi, K. K. Kim, A. Reina, M. Hofmann, L. J. Li, and J. Kong, *ACS Nano*, 2010, **5**, 2689–2694..
63. L. Gomez De Arco, Y. Zhang, C. W. Schlenker, K. Ryu, M. E. Thompson, and C. Zhou, *ACS Nano*, 2010, **4**, 2865–2873.
64. P. Avouris, *Nano Lett.*, 2010, **10**, 4285–4294.
65. Y. Shi, W. Fang, K. Zhang, W. Zhang, and L. J. Li, *Small*, 2009, , 2005–2011.

66. S. Bae, H. Kim, Y. Lee, X. Xu, J. S. Park, Y. Zheng, J. Balakrishnan, T. Lei, H. R. Kim,Y. Song, Y. J. Kim, K. S. Kim, B. Ozyilmaz, J. H. Ahn, B. H. Hong, and S. Iijima, *Nat. Nanotechnol.*, 2010, **5**, 574–578.

67. J. R. Durán Retamal, C. F. Kang, C. H. Ho, J. J. Ke, W. Y. Chang and J. H. He, *Appl. Phys. Lett.,* 2014, **105**, 253111.

68. C. Y. Chen, M. W. Chen, J. J. Ke, C. A. Lin, J. R. D. Retamal and J. H. He, *Pure Appl. Chem.* 2010, **82**, 2055-2073.

69. Y. Hu, J. Zhou, P. H. Yeh, Z. Li, T. Y. Wei, Z. L. Wang, *Adv. Mater.* 2010, **22**, 3327–3332.

70. J. H. He, P. H. Chang, C. Y. Chen, K. D. Tsai, *Nanotechnology*, 2009, **20**, 135701.

71. P. C. Chen, G. Shen, C. Zhou, *IEEE Trans. Nanotechnol.* 2008, **7**, 668–682.

72. P. S. Cho, K. W. Kim and J. H. Lee, *J. Electroceram.* 2006, **17**, 975–978.

73. G. S. Devi, V. B. Subrahmanyam, S. C. Gadkari and S. K. Gupta, *Anal. Chim. ACTA*, 2006, **568**, 41–46.

74. H. Gong, J. Q. Hu, J. H. Wang, C. H. Ong and F. R. Zhu, *Sens. Actuators B, Chem.* 2006, **115**, 247–251.

75. H. T. Wang, B. S. Kang, F. Ren, L. C. Tien, P. W. Sadik, D. P. Norton, S. J. Pearton and J. Lin, *Appl. Phys. Lett.* 2005, **86**, 243503.

76. X. H. Wang, Y. F. Ding, J. Zhang, Z. Q. Zhu, S. Z. You, S. Q. Chen and J. Z. Zhu, *Sens. Actuators B, Chem.* 2006, **115**, 421–427.

77. S. Christoulakis, M. Suchea, E. Koudoumas, M. Katharakis, N. Katsarakis and G. Kiriakidis, *Appl. Surface Sci.* 2006, **252**, 5351–5354.

78. C. H. Wang, X. F. Chu and M. W. Wu, *Sens. Actuators B, Chem.* 2006, **113**, 320–323.

79. T. F. Xue, J. F. Hu, H. W. Qin, Y. Zhou, K. An, L. Zhang, T. Han and Y. X. Li, *Rare Metal Mater. Eng.* 2004, 33, 1006–1008.

80. E. Comini, C. Baratto, G. Faglia, M. Ferroni and G. Sberveglieri, *J. Phys. D* 2007, **40**, 7255-7259.

81. Q. H. Li, Y. X. Liang, Q. Wan and T. H. Wang, *Appl. Phys. Lett.* 2004, **85**, 6389-6391.

82. Z. Y. Fan, D. W. Wang, P. C. Chang, W. Y. Tseng and J. G. Lu, *Appl. Phys. Lett.* 2004, **85**, 5923-5925.

83. C. Y. Lu, S. P. Chang, S. J. Chang, T. J. Hsueh, C. L. Hsu, Y. Z. Chiou, C. Chen, *IEEE Sens. J.* 2009, **9**, 485-489.

84. E. Comini, G. Faglia, G. Sberveglieri, Z. W. Pan, Z. L. Wang, *Appl. Phys. Lett.* 2002, **81**, 1869-1871.

85. G. Kwak, K. J. Yong, J. Phys. Chem. C 2008, 112, 3036–3041.

86. R. K. Joshi, Q. Hu, F. Am, N. Joshi and A. Kumar, *J. Phys. Chem. C* 2009, **113**, 16199–16202.

87. T. J. Hsueh, Y. W. Chen, S. J. Chang, S. F. Wang, C. L. Hsu, Y. R. Lin, T. S. Lin, I. C. Chen, *J. Electrochem. Soc.* 2007, **154**, J393-J396.

88. L. Liao, H. B. Lu, J. C. Li, C. Liu, D. J. Fu, Y. L. Liu, *Appl. Phys. Lett.* 2007, **91**, 173110.

89. L. C. Tien, P. W. Sadik, D. P. Norton, L. F. Voss, S. J. Pearton, H. T. Wang, B. S. Kang, F. Ren, J. Jun and J. Lin, *Appl. Phys. Lett.* 2005, **87**, 222106.

90. Q. Wan, Q. H. Li, Y. J. Chen, T. H. Wang, X. L. He, J. P. Li and C. L. Lin, *Appl. Phys. Lett.* 2004, **84**, 3654-3656.

91. J. S. Park, W.-J. Maeng, H.-S. Kim and J.-S. Park, *Thin Solid Films*, 2012, **520**, 1679-1693.

92. E. Fortunato, P. Barquinha and R. Martins, *Adv. Mater.*, 2012, **24**, 2945-2986.

93. L. Wei, X. Ping and C. M. Lieber, *IEEE Trans. Electron Dev.*, 2008, **55**, 2859-2876.

94. R. JoséRamónDurán, C. Cheng-Ying, L. Kun-Yu and H. Jr-Hau, in *Handbook of Zinc Oxide and Related Materials*, Taylor & Francis2012, pp. 133-174.

95. K. Nomura, H. Ohta, K. Ueda, T. Kamiya, M. Hirano and H. Hosono, *Science*, 2003, **300**, 1269-1272.

96. K. Nomura, H. Ohta, A. Takagi, T. Kamiya, M. Hirano and H. Hosono, *Nature*, 2004, **432**, 488-492.

97. J. F. Conley, *IEEE Trans. Electron Dev.*, 2010, **10**, 460-475.

98. J. K. Jeong, H. Won Yang, J. H. Jeong, Y.-G. Mo and H. D. Kim, *Appl. Phys. Lett.*, 2008, **93**, 3513.

99. D. Kang, H. Lim, C. Kim, I. Song, J. Park, Y. Park and J. Chung, *Appl. Phys. Lett.*, 2007, **90**, 192101.

100. C. Ming-Wei, J. R. D. Retamal, C. Cheng-Ying and H. Hau, *Electron Device Letters, IEEE*, 2012, **33**, 411-413.

101. M. E. Lopes, H. L. Gomes, M. C. R. Medeiros, P. Barquinha, L. Pereira, E. Fortunato, R. Martins and I. Ferreira, *Appl. Phys. Lett.* 2009, **95**, 063502.

102. Y.-C. Chen, T.-C. Chang, H.-W. Li, T.-Y. Hsieh, T.-C. Chen, C.-P. V., C.-H. Chou, W.-C. Chung, J.-F. Chang and Y.-H. Tai, *Appl. Phys. Lett.* 2012, **101**, 041908.

103. P. Liu, T. P. Chen, X. D. Li, Z. Liu, J. I. Wong, Y. Liu and K. C. Leong, *Appl. Phys. Lett.*, 2013, **103**, 202110.

104. K. Takechi, M. Nakata, T. Eguchi, H. Yamaguchi and S. Kaneko, *J. Appl. Phys.*, 2009, **48**, 010203.

105. S. P. Chang, B.-K. Ju, J. *Adv. Smart Convergence*, 2012, **1**, 61-64.

Author Photograph(s)

Der-Hsien Lien received B.S. degree (2003)and the M.S. degree (2005) in the Department of Materials Science and Engineering from National Tsing Hua University. He is a Ph.D. student in the Institute of Electronics Engineering at National Taiwan University, and currently works in the Electrical Engineering & Computer Sciences, UC Berkeley as a visiting scholar. His research interests include the nanophotonics dynamics and applications, 2D materials electronics and photonics, random access resistive memories, and flexible optoelectronics. Currently he has authored 35 peer-reviewed journal papers, holds 1 US patent and 2 Taiwan patents.

José Ramón Durán Retamal received his B.S. and M.S. degree (2007) from the Telecommunication Engineering School, Technical University of Madrid. He received his Ph.D. degree (2014) from Graduate Institute of Photonics and Optoelectronics at the National Taiwan University. Currently, he is a postdoctoral fellow at the Computer, Electrical and Mathematical Sciences and Engineering Division of King Abdullah University of Science and Technology (KAUST). His research activities include metal oxide nanostructures with applications in electronics, bio-sensing and optoelectronics. He also work on the fabrication of 3D vertical resistive random-access memory devices and its applications.

Chen-Fang Kang received the B.S. in Department of Physics at Tunghai University, Taichung, Taiwan. Then, he received his M.S. degree at National Chung Cheng University, Chiayi, Taiwan. He is currently a Ph.D. student at the Graduate Institute of Photonics and Optoelectronics, National Taiwan University, Taipei, Taiwan. He has dedicated to research in non-linear optics and focused on exploring the resistive switching properties of novel ternary oxides.

Jr-Jian Ke received the B.S. degree in electrical engineering from National University of Kaohsiung, Taiwan, in 2007 and the M.S. degree Graduate Institute of Photonics and Optoelectronics, National Taiwan University, Taipei, Taiwan, in 2009 where he is currently working toward the Ph.D..His past research actives includes the transport mechanism of nanowires and metal-semiconductor interface. He is now working on the fabrication, transport modeling of the resistive random-access memory devices and their applications
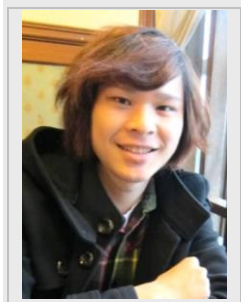
Jr-Hau He received his B.S. and Ph.D. degrees from the National Tsing Hua University, Hsinchu, Taiwan, in 1999 and 2005, respectively. He is currently an Associate Professor of King Abdullah University of Science and Technology (KAUST). He is involved in the design of new nanostructured architectures for nanophotonics and the next generation of nanodevices, including photovoltaics, and resistive memory. Prof. He is a recipient of the Outstanding Young Electrical Engineer Award from the Chinese Institute of Electrical Engineering (2013), the Outstanding Youth Award of the Taiwan Association for Coating and Thin Film Technology (2012), the Youth Optical Engineering Medal of the Taiwan Photonics Society (2011), and has won numerous other awards and honors with his students in professional societies and conferences internationally.

The surface effect can be either a negative or beneficial effect on nanodevices depending on the environmental conditions and device applications. This review provides an introduction of the surface effects on different types of nanodevices, offering the solutions to response to their benefits and negative effect, and provides outlooks on further applications regarding the surface effect, which is beneficial for designing nano-enabled photodetectors, memories, sensors and transistors via surface engineering.

Der-Hsien Lien, José Ramón Durán Retamal, Chen-Fang Kang, Jr-Jian Ke and Jr-Hau Hea*

Surface Effects in Metal Oxide-Based Nanodevices